Friction **10**(12): 2018–2032 (2022)
https://doi.org/10.1007/s40544-021-0568-3
ISSN 2223-7690
CN 10-1237/TH
RESEARCH ARTICLE

Synergistic lubrication of few-layer $Ti_3C_2T_x$/MoS_2 heterojunction as a lubricant additive

Peng FENG[1], **Yanping REN**[2], **Yuting LI**[1], **Jifan HE**[2], **Zhuang ZHAO**[1], **Xiaoliang MA**[1], **Xiaoqiang FAN**[1,*], **Minhao ZHU**[1,2]

[1] *Key Laboratory of Advanced Technologies of Materials (Ministry of Education), School of Materials Science and Engineering, Southwest Jiaotong University, Chengdu 610031, China*

[2] *Tribology Research Institute, School of Mechanical Engineering, Southwest Jiaotong University, Chengdu 610031, China*

Received: 19 July 2021 / Revised: 31 August 2021 / Accepted: 02 November2021

Abstract: The few-layer $Ti_3C_2T_x$/MoS_2 heterostructure was successfully prepared via vertically growing of MoS_2 nanosheets on the few-layer $Ti_3C_2T_x$ matrix using hydrothermal method. The tribological properties as additive in mineral oil (150N) were evaluated in detail. The 0.3 wt% of few-layer $Ti_3C_2T_x$/MoS_2 heterostructure addition amount can reduce the friction and wear of 150N by 39% and 85%, respectively. Moreover, the enhancement effect of few-layer $Ti_3C_2T_x$/MoS_2 on tribological properties of 150N is superior to that of few-layer $Ti_3C_2T_x$, MoS_2 nanosheets, and their mechanical mixture. Based on the characterization and analysis of wear debris and wear track, such excellent tribological properties of the few-layer $Ti_3C_2T_x$/MoS_2 heterostructure derive from its structural advantage toward good dispersion, the synergistic lubrication of $Ti_3C_2T_x$ and MoS_2 nanosheets during the rubbing process, and the formation of tribo-film.

Keywords: few-layer $Ti_3C_2T_x$; molybdenum disulfide (MoS_2); heterojunction; tribological performance

1 Introduction

In the wake of the development of mechanical equipment, friction and wear of moving elements cause serious energy consumption and material losses. Therefore, reducing friction and wear is still currently a top priority [1–4]. Use of lubricating oil is one of the effective ways for friction reduction and wear resistance. Unfortunately, traditional lubricating oil can no longer meet the ever-increasing performance requirements under extremely working conditions. Recently, a series of functional additives have been developed to improve lubrication performance, like nanomaterials [5, 6], ionic liquids [7, 8], and polymers [9], etc. In terms of these functional additives, the two-dimensional (2D) nanomaterials have been broadly introduced into lubricants [10–13], like graphene, molybdenum disulfide (MoS_2), boron nitride, and so on.

MXene, as a novel 2D material, has received considerable attention since the first discovered by Drexel University scientists in 2011 [14]. MXenes are prepared by selected etching the "A" layer from layered ternary compound $M_{n+1}AX_n$ (n = 1, 2, or 3) phases, where "M" is an early transition metal (e.g., Ti, Nb, Mo, Cr, and so on), "A" represents a group IIIA or IVA element, and "X" is C and/or N. $Ti_3C_2T_x$, as a kind of typical MXene material, has been extensively investigated for sensors, catalysts, lithium ion batteries, electrochemical capacitors, and other fields due to the rich chemistries and unique morphologies [15–21]. In addition, because of its outstanding mechanical strength, layered graphene-like structure, and low shear strength, $Ti_3C_2T_x$ is a highly potential additive to improve the lubrication properties. Zhang et al. [22] early investigated the tribological performance of $Ti_3C_2T_x$ as lubricant additive,

* Corresponding author: Xiaoqiang FAN, E-mail: fxq@home.swjtu.edu.cn

and proved that $Ti_3C_2T_x$ at the optimal concentration could positively improve the friction reduction and anti-wear due to the easily-shearing $Ti_3C_2T_x$ nanosheets and tribofilm on the sliding interfaces. Liu et al. [23] reported the effect of exfoliation degree on tribological properties of multilayer $Ti_3C_2T_x$ as a lubricating additive. The results proved that $Ti_3C_2T_x$ with a high exfoliation degree has excellent friction-reducing and anti-wear abilities. Nguyen et al. [24] reported that multilayer $Ti_3C_2T_x$ sheets as additives in water-based lubrication, exhibit remarkable enhancement in anti-friction and wear-resistant abilities. The above researches showed that even a small amount of $Ti_3C_2T_x$ could significantly improve the tribological performance of the fluid. Zhao et al. [25] measured the lubrication performance of graphene additives with different layer numbers, and few-layer graphene has better lubrication properties than multilayer graphene, as few-layer graphene can form an ordered tribofilm which parallels to the sliding direction at friction interface. Therefore, few-layer $Ti_3C_2T_x$ similar to few-layer graphene may also show good lubrication performance. However, when few-layer $Ti_3C_2T_x$ nanosheets were applied as lubricant additive, they tend to agglomerate because of their plentiful polar groups and high specific surface energy [26]. Therefore, a feasible way on overcoming the compatibility of nano-additives in oil is to synthesize the $Ti_3C_2T_x$-based nanocomposite with unique structure for inhibiting agglomeration.

In previous researches, MoS_2 has been demonstrated outstanding friction-reducing and anti-wear abilities as a lubricant additive due to the feeble van der Waals force between the interlayers and the strong covalent bonding within the intramolecular [27–29]. Chouhan et al. [30] reported that the reduced graphene oxide/MoS_2 heterostructure as an oil additive displays excellent synergistic lubricating behaviors. Interestingly, with the introduction of curved MoS_2 structure, the reduced graphene oxide/MoS_2 heterostructure is easier for dispersion in base oil [30–32]. In addition, small size MoS_2 nanosheets can be uniformly grown on few-layer $Ti_3C_2T_x$ matrix. So MoS_2 is a good candidate for preparing $Ti_3C_2T_x$-based nanocomposite to improve the tribological properties of few-layer $Ti_3C_2T_x$.

In this study, few-layer $Ti_3C_2T_x$ was prepared by the adjusted minimally intensive layer delamination method [33]. Then, few-layer $Ti_3C_2T_x/MoS_2$ heterojunction was synthesized by hydrothermal method. The tribological performance of $Ti_3C_2T_x/MoS_2$ heterojunction in mineral oil (150N) was tested by a UMT-3 tribotester, and its lubricant mechanism was further investigated. By comparing the lubrication properties of $Ti_3C_2T_x$, MoS_2, and their mechanical mixture, the synergistic effect of heterojunction was explored, and a probable lubrication mechanism was proposed according to the results.

2 Experimental details

2.1 Materials

Ti_3AlC_2 powder was provided by Ningbo Beijiaer New Material Co., Ltd., China. $(NH_4)_6Mo_7O_{24}\cdot 4H_2O$, HCl, LiF, thiourea, absolute ethyl alcohol, acetone, and other chemical reagents were purchased from Chengdu Kelong Chemical, China. All chemical reagents were directly used without further purification. Deionized water was synthesized in the laboratory.

2.2 Preparation of few-layer $Ti_3C_2T_x$

The synthesis of few-layer $Ti_3C_2T_x$ draws lessons from the minimally intensive layer delamination synthesis method. First, 20 mL 9M HCl and 1.6 g LiF were added to the PTFE reactor, and the mixture was continually stirred at room temperature until LiF particles were fully dissolved to form an etchant. Then, 1 g Ti_3AlC_2 was carefully and slowly added to the above etchant within 5 min to dissipate initial overheating caused by exothermic nature of the reaction. After that, the obtained suspension was continuously stirred at 35 °C for 24 h. Subsequently, the resulting acidic suspension was repeatedly centrifuged and washed with deionized water until the suspension reached a pH of about 7. The black sediment at the bottom of the centrifuge tube, containing $Ti_3C_2T_x$ and non-etched Ti_3AlC_2, was collected and cautiously moved into a 300 mL beaker containing 150 mL deionized water. The dispersion was treated by ultrasonication in ice water under a N_2 atmosphere for 30 min. Finally, the dispersion after ultrasonication was centrifuged at 5,000 rpm for 10 min, and the supernatant containing few-layer $Ti_3C_2T_x$ was carefully obtained and dried.

2.3 Preparation of few-layer $Ti_3C_2T_x/MoS_2$ heterojunction

Few-layer $Ti_3C_2T_x/MoS_2$ heterojunction was synthesized by hydrothermal method. Firstly, 0.7062 g $(NH_4)_6Mo_7O_{24}\cdot 4H_2O$ and 1.5224 g thiourea were gradually submerged in 20 mL of deionized water by ultrasound for 30 min to get a homogeneous solution. Then, 0.1173 g few-layer $Ti_3C_2T_x$ powder was dissolved in the solution by ultrasound for 30 min. The mixture was carefully transferred to a 50 mL Teflon-lined stainless-steel autoclave and hydrothermally treated at 210 °C for 18 h in the drying oven. After the reaction, the resultant product was repeatedly centrifuged, washed, and dried to obtain few-layer $Ti_3C_2T_x/MoS_2$ heterojunction.

2.4 Characterizations

X-ray diffraction (XRD, Rigaku Smartlab, Japan) patterns were performed to characterize crystallinity and phase structure of samples with Cu Kα radiation (U = 40 kV, I = 40 mA, and λ = 0.154 nm). The microstructure and morphology of samples were characterized using a field-emission scanning electron microscopy (SEM, FEI Inspect F50, USA). Raman spectra (DXR, Thermo Fisher, USA) was excited with a 532 nm excitation laser and X-ray photoelectron spectrometer (XPS, ESCALAB 250Xi, USA) were performed to observe chemical composition and chemical state of samples. Atomic force microscope (AFM, FM-Nanoview1000AFM, China) was measured to characterize the height profiles of the few-layer $Ti_3C_2T_x$.

2.5 Friction and wear performances

In the friction tests, mineral oil (150N) was selected as base oil. The prepared additives were dispersed into the 150N by stirring and ultrasonic treatment for 5 min. The tribological behaviors of samples were evaluated using the ball-on-plate friction tests on the multi-function reciprocating sliding tribometer (CETR UMT-3, USA) under the condition of drying in air. In addition, the counterpart ball and lower steel substrates were GCr15 bearing steel with the hardness of 710 HV and the surface roughness of Ra = 50 nm. The counterpart balls were cleaned by an ultrasonic bath in acetone before testing. And the sliding amplitude, oscillation frequency, and duration of every experiment were 1 mm, 5 Hz, and 60 min, respectively. White light interferometer (Bruker Contour GT, Germany) was used to obtain the wear volume of wear track. The chemical state and morphologies of the friction surface were characterized by X-ray photoelectron spectrometer (XPS, ESCALAB 250Xi, USA) and field-emission scanning electron microscopy (SEM, FEI Inspect F50, USA). To further explore the nanostructure transformation of few-layer $Ti_3C_2T_x/MoS_2$ heterojunction after friction tests, the wear debris was carefully collected and cleaned for analysis.

3 Results and discussion

3.1 Chemical and structural characterization of nanomaterials

The synthesis process of few-layer $Ti_3C_2T_x/MoS_2$ heterojunction is depicted in Fig. 1. First, Ti_3AlC_2 powders were etched in an etchant composed of LiF salts and HCl solution to get multilayer $Ti_3C_2T_x$. Then, few-layer $Ti_3C_2T_x$ was obtained with the assistance of appropriate ultrasonication. Finally, the few-layer $Ti_3C_2T_x$ was dispersed in a clear solution containing $(NH_4)_6Mo_7O_{24}\cdot 4H_2O$ and thiourea to synthesize few-layer $Ti_3C_2T_x/MoS_2$ heterojunction using hydrothermal method. During the hydrothermal preparation process, the oxygen-containing functional groups on the surface of few-layer $Ti_3C_2T_x$ can be used as sites for the growth of MoS_2, and the MoS_2 nanosheets are vertically and uniformly grown on the surface of few-layer $Ti_3C_2T_x$ [34].

SEM images of multilayer $Ti_3C_2T_x$, MoS_2, few-layer $Ti_3C_2T_x$, and few-layer $Ti_3C_2T_x/MoS_2$ heterostructure are shown in Figs. S1 and S2 in the Electronic Supplementary Material (ESM) and Figs. 2(a)–2(c). The pure MoS_2 sample (Fig. S1 in the ESM) is composed of MoS_2 nanosheets, which aggregates into a spherical shape due to the lack of $Ti_3C_2T_x$ as a matrix. After LiF and HCl etching Al layers, the Ti_3AlC_2 with bulk structure is successfully transformed into a typical organ-like $Ti_3C_2T_x$ structure, which indicates the successful removal of the Al atomic layer (Fig. S2 in

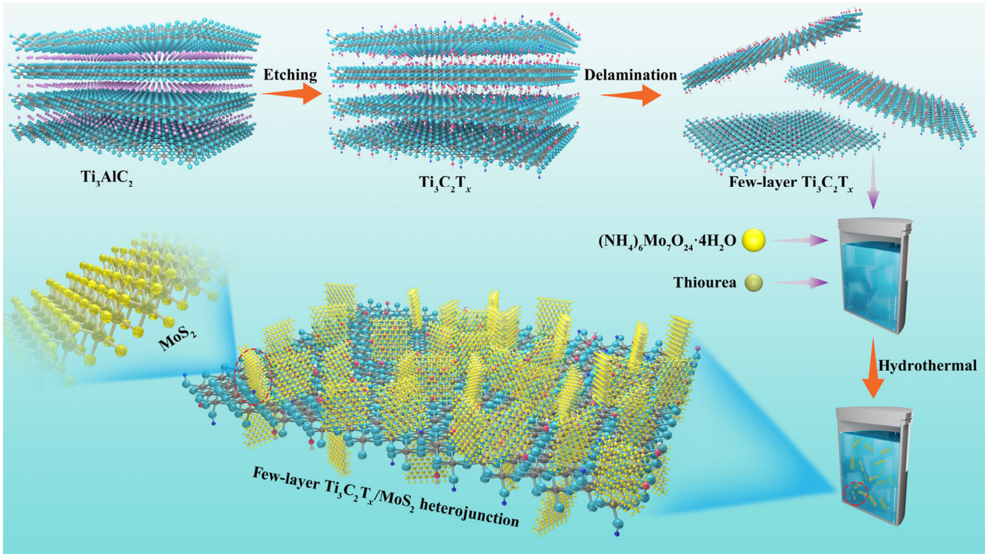

Fig. 1 Schematic illustration on synthesis of few-layer $Ti_3C_2T_x/MoS_2$ heterojunction.

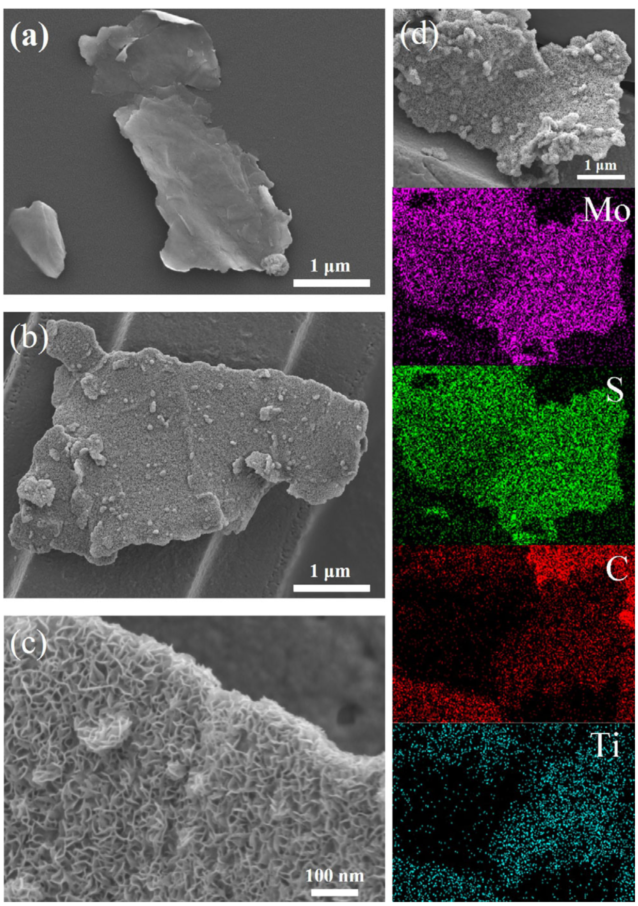

Fig. 2 SEM images of (a) few-layer $Ti_3C_2T_x$ and (b, c) few-layer $Ti_3C_2T_x/MoS_2$ heterostructure. (d) Elemental mapping images of few-layer $Ti_3C_2T_x/MoS_2$ heterostructure.

the ESM). It is obvious that the few-layer $Ti_3C_2T_x$ (Fig. 2(a)) is successfully obtained by the ultrasonication of multilayer $Ti_3C_2T_x$ dispersion, and the number of layers is significantly reduced. Compared with multilayer $Ti_3C_2T_x$, the few-layer $Ti_3C_2T_x$ has a larger specific surface area, which can provide more matrices for the growth of MoS_2 nanosheets to alleviate the agglomeration of MoS_2 nanosheets. After the hydrothermal reaction, MoS_2 nanosheets are vertically and uniformly grown on the few-layer $Ti_3C_2T_x$ matrix to synthesize few-layer $Ti_3C_2T_x/MoS_2$ heterostructure (Figs. 2(b) and 2(c)). The *in situ* generated MoS_2 is tightly bound to the few-layer $Ti_3C_2T_x$, which reduces the agglomeration of MoS_2 nanosheets and expands the few-layer $Ti_3C_2T_x$ layer spacing. As shown in Fig. 2(d), elemental mapping images further show the uniform distribution of Mo, S, Ti, and C in entire the few-layer $Ti_3C_2T_x/MoS_2$ heterostructure, suggesting that MoS_2 was uniformly attached on the few-layer $Ti_3C_2T_x/MoS_2$ heterostructure surface in the form of nanosheets.

In order to further prove that the prepared $Ti_3C_2T_x$ is few-layer $Ti_3C_2T_x$, the thickness of the $Ti_3C_2T_x$ is investigated by atomic force microscopy (AFM). AFM height profile in Fig. 3 shows the $Ti_3C_2T_x$ with a thickness of about 4.7 nm. It is well known that the thickness of a monolayer $Ti_3C_2T_x$ is 0.98 nm, and the adsorbed water also contributes to the thickness [35–37]. Therefore, the 4.7-nm-thick flake should be three layers structures, which indicates that few-layer $Ti_3C_2T_x$ has been successfully prepared.

The crystalline structures, chemical composition,

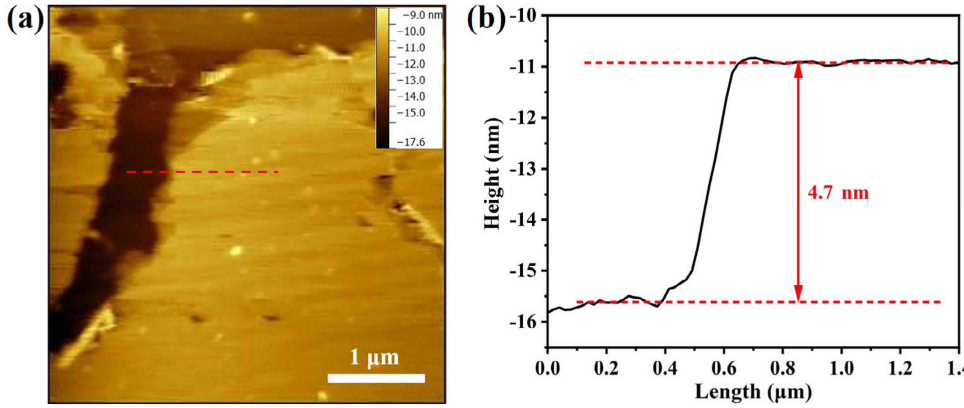

Fig. 3 (a) AFM image and (b) corresponding height profile of few-layer $Ti_3C_2T_x$.

and chemical state of the samples were investigated using XRD, Raman spectra, and XPS in Fig. 4. Figure 4(a) shows the characteristic peaks in the XRD patterns of few-layer $Ti_3C_2T_x$, MoS_2, and few-layer $Ti_3C_2T_x/MoS_2$ heterostructure. The diffraction peaks at 2θ of 9.4°, 32.3°, and 57.8° correspond to the (002), (100), and (110) planes of MoS_2, respectively, demonstrating the formation of a layered structure of MoS_2 [38]. After etching and delamination, the characteristic peaks at 6.7°, 34.5°, 38.9°, and 60.8° can be indexed to the (002), (0010), (0012), and (110) planes of few-layer $Ti_3C_2T_x$, respectively [39, 40]. The diffraction peaks of MoS_2 can be clearly observed in the few-layer $Ti_3C_2T_x/MoS_2$ heterostructure. However, the (002) plane of few-layer $Ti_3C_2T_x$ does not appear in the heterojunction. Possible factors are that the intercalation of MoS_2 and NH_4^+ during hydrothermal synthesis leads to a lower angle deviation of the (002), so no peaks are captured in 5°–80° [41]. The hydrothermal reaction causes the partial oxidation of $Ti_3C_2T_x$ and the formation of TiO_2, so the XRD peak located at 25.2° can be attributed to the (101) peak of TiO_2 [42].

The Raman spectra of the few-layer $Ti_3C_2T_x$, MoS_2, and few-layer $Ti_3C_2T_x/MoS_2$ heterostructure are shown in Fig. 4(b). The typical modes of few-layer $Ti_3C_2T_x$ are clearly observed. The characteristic peaks appearing at 406 and 609 cm^{-1} can be indexed to the $Ti_3C_2T_x$, indicating the successful preparation of few-layer $Ti_3C_2T_x$ [43]. The prepared MoS_2 and few-layer $Ti_3C_2T_x/MoS_2$ heterostructure show two strong characteristic peaks at 371 and 397 cm^{-1}, which can be indexed to typical E^1_{2g} and A_{1g} peaks of MoS_2, suggesting that the pure MoS_2 and few-layer $Ti_3C_2T_x/MoS_2$ heterostructure were successfully produced by hydrothermal route [44]. As the laser cannot penetrate through the MoS_2 nanosheets on the surface of $Ti_3C_2T_x$ nanosheets, so showing no characteristic peaks of underlying $Ti_3C_2T_x$ nanosheets in the few-layer $Ti_3C_2T_x/MoS_2$ heterojunction. Therefore, the Raman spectra of MoS_2 and few-layer $Ti_3C_2T_x/MoS_2$ heterojunction are familiar.

The XPS analysis of few-layer $Ti_3C_2T_x/MoS_2$ heterostructure is investigated and the test result is shown in Fig. 4(c). The full-scale XPS pattern of few-layer $Ti_3C_2T_x/MoS_2$ heterostructure reveals that

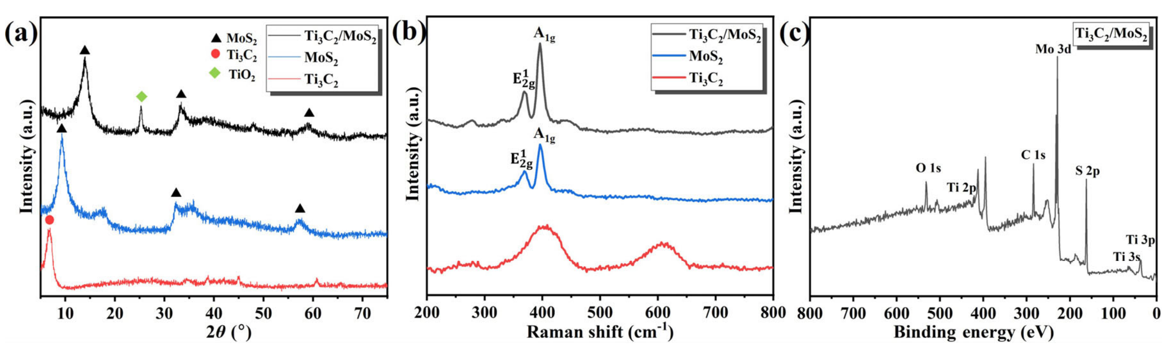

Fig. 4 (a) XRD patterns of few-layer $Ti_3C_2T_x$, MoS_2, and few-layer $Ti_3C_2T_x/MoS_2$ heterostructure. (b) Raman spectra of the $Ti_3C_2T_x$, MoS_2, and few-layer $Ti_3C_2T_x/MoS_2$ heterostructure. (c) XPS fully scanned spectra of few-layer $Ti_3C_2T_x/MoS_2$ heterostructure.

Mo, S, Ti, C, and O are the predominant elements and no other impurity elements, which further manifests the high purity of the few-layer $Ti_3C_2T_x/MoS_2$ heterostructure.

3.2 Tribological performance of lubricant additives

The friction coefficient and wear volume of dispersions of 150N with different concentrations of few-layer $Ti_3C_2T_x/MoS_2$ heterojunction are shown in Fig. 5. The friction coefficient of pure 150N showed a gradual rise and then tended to considerably fluctuate around 0.14, which possibly emerged the direct contact on the wear surface under the boundary lubricating condition. However, using the few-layer $Ti_3C_2T_x/MoS_2$ heterojunction as an additive greatly improved the tribological properties of the 150N. In the concentration range of 0.1–0.9 wt%, the friction coefficient and wear volume of 150N with additives are lower than those of pure 150N. In addition, with the adding of few-layer $Ti_3C_2T_x/MoS_2$ heterojunction, the friction coefficient curve will eventually smooth and stabilize after the initially slight fluctuation, which is obviously different from the friction coefficient curve of 150N without additives. The above results show that the few-layer $Ti_3C_2T_x/MoS_2$ heterojunction has a good tribological performance. As the increase of added concentration, the average friction coefficient first decreases and then increases. When the concentration is less than 0.3 wt%, the tribological performance is poor because the amount of nano additives is not enough to support the formation of a uniform and dense friction film between the pair of grinding pairs; When the concentration is greater than 0.3 wt%, the heterojunction is prone to agglomeration and cannot enter the friction interface, which leads to poor tribological performance. From the above experiment, the results show that few-layer $Ti_3C_2T_x/MoS_2$ heterojunction has the first-class friction-reducing and anti-wear abilities at an addition amount of 0.3 wt%. So, subsequent experiments selected an additive concentration of 0.3 wt%.

To comprehensively evaluate the lubricating performance of few-layer $Ti_3C_2T_x/MoS_2$ heterojunction under different loads, friction tests were also performed at 20, 60, 100, and 140 N in Fig. 6. The results showed that, compared to pure base oil without additives, the mean friction coefficient of the lubricants with heterojunction additives was reduced by 27.9%, 31.7%, 32.8%, and 38.9% under 20, 60, 100, and 140 N loads, respectively. Obviously, as the load increases, the effect of friction reduction gets better and better. The reason may be that it is easier to form a stable tribochemical film under the high loads. As can be seen from Fig. S3 in the ESM, compared with base oil, the lubricants with the heterojunction additives can make the friction curve more stable under different loads. The reason may be that the few-layer $Ti_3C_2T_x/MoS_2$ heterojunction formed a stable tribofilm on the surface of counterpart. It is obvious that the few-layer $Ti_3C_2T_x/MoS_2$ heterojunction improved the tribological performance of 150N at different loads, which should benefit from the good synergistic lubrication performance of few-layer $Ti_3C_2T_x/MoS_2$ heterojunction.

In order to investigate the synergistic effect of few-layer $Ti_3C_2T_x/MoS_2$ heterojunction, the friction coefficient curves and wear volume of few-layer

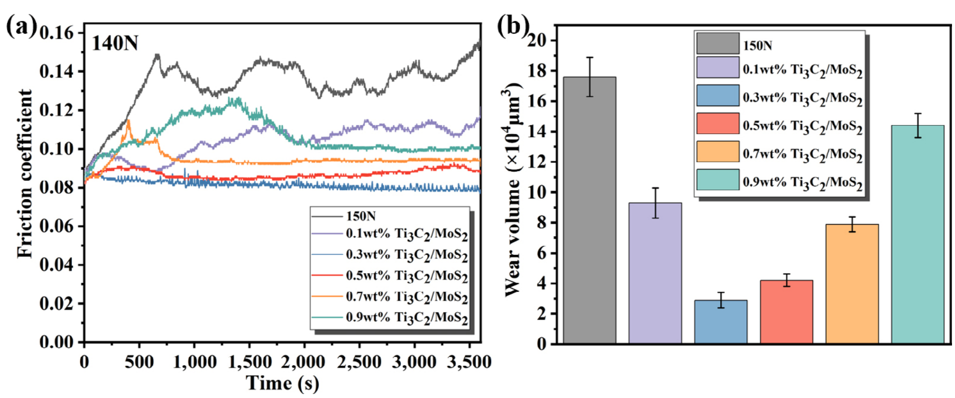

Fig. 5 (a) Friction coefficient curves and (b) wear volumes lubricated by 150N with few-layer $Ti_3C_2T_x$ heterojunction additive at different concentrations.

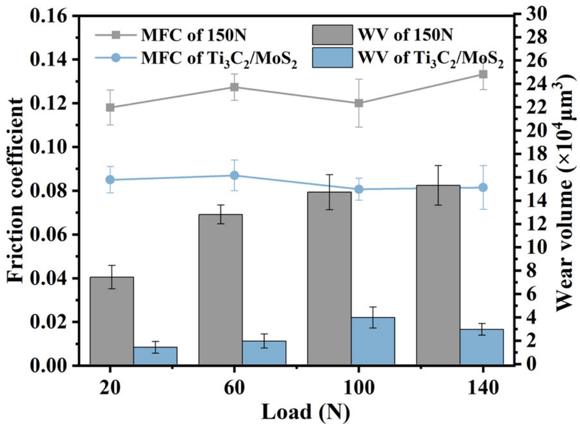

Fig. 6 Variations of the mean friction coefficient and wear volumes lubricated by few-layer $Ti_3C_2T_x/MoS_2$ heterojunction with the increasing load.

$Ti_3C_2T_x/MoS_2$ heterojunction were compared with pure few-layer $Ti_3C_2T_x$, MoS_2, and their mechanical mixture (Fig. 7). Under the load of 140 N, the average friction coefficient of 150N, few-layer $Ti_3C_2T_x$, MoS_2, $Ti_3C_2T_x/MoS_2$ mixture, and few-layer $Ti_3C_2T_x/MoS_2$ heterojunction are 0.1332, 0.1222, 0.1093, 0.1438, and 0.0814, respectively. Figure 7 shows that except for mechanical mixture, all other additives in 150N can reduce the friction coefficient and wear volume. The friction coefficient and wear volume of pure few-layer $Ti_3C_2T_x$ are not significantly reduced, which may be caused by the fact that the load-bearing capacity of few-layer $Ti_3C_2T_x$ is not good and the few-layer $Ti_3C_2T_x$ is easier to agglomerate due to its plentiful polar groups and high specific surface energy [26, 45]. Compared with pure few-layer $Ti_3C_2T_x$, pure MoS_2 exhibits better performance. This is because MoS_2 is a recognized 2D layered lubricating additive, which can have better tribological properties under high loads, being consistent with previous studies [46, 47]. Apparently, the few-layer $Ti_3C_2T_x/MoS_2$ heterojunction additive exhibits the smallest wear volumes (decreased by 83.52%) and lowest friction coefficient (decreased by 38.85%). In addition, compared with unstable and fluctuate friction curve of other additives, the heterojunction has a more smooth and stable friction curve and lower average friction coefficients. Therefore, the few-layer $Ti_3C_2T_x/MoS_2$ heterojunction has superior tribological performance than individual few-layer $Ti_3C_2T_x$ or MoS_2, which benefits from the synergistic lubrication of few-layer $Ti_3C_2T_x$ and MoS_2 nanosheets in the heterojunction.

The three-dimensional (3D) morphologies, cross-sectional profile, and SEM images were investigated to intuitively observe the wear surface of the steel discs lubricated with pure 150N and 150N containing 0.3 wt% of the few-layer $Ti_3C_2T_x$, MoS_2, $Ti_3C_2T_x/MoS_2$ mixture, and few-layer $Ti_3C_2T_x/MoS_2$ heterojunction and the results are shown in Fig. 8. Obviously, the wear track lubricated with pure 150N is the deepest (Fig. 8(a_1)), and there are many furrows on the wear surface (Fig. 8(a_4)), demonstrating the serious adhesion wear. In addition, the wear tracks lubricated with $Ti_3C_2T_x$, MoS_2, and mechanical mixture describe slight abrasive wear. Compared with the $Ti_3C_2T_x$, MoS_2, and their mechanical mixture, the wear track lubricated with 150N containing few-layer $Ti_3C_2T_x/MoS_2$ heterojunction shows the shallowest and smoothest wear surface (Figs. 8(e_1)–8(e_4)), which also reflects the extremely excellent synergistic lubrication effect of $Ti_3C_2T_x$ and MoS_2 in the heterojunction.

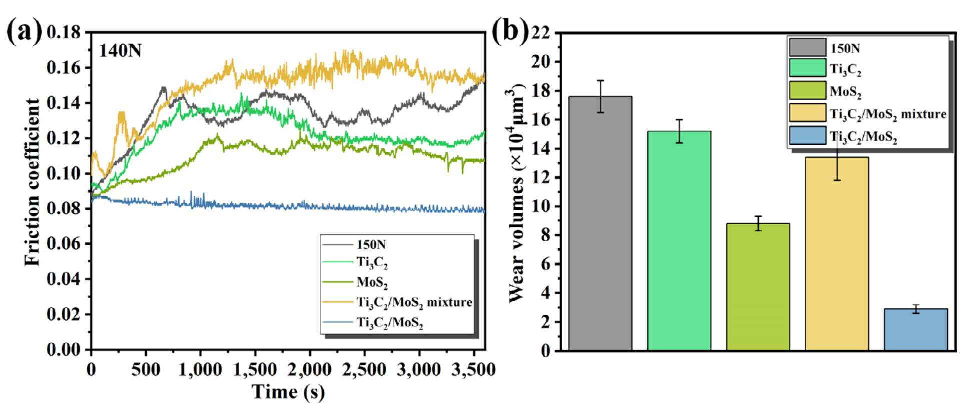

Fig. 7 (a) Friction coefficient curves and (b) wear volumes lubricated by 150N with Ti_3C_2, MoS_2, Ti_3C_2/MoS_2 mixture, and few-layer $Ti_3C_2T_x/MoS_2$ heterojunction additive.

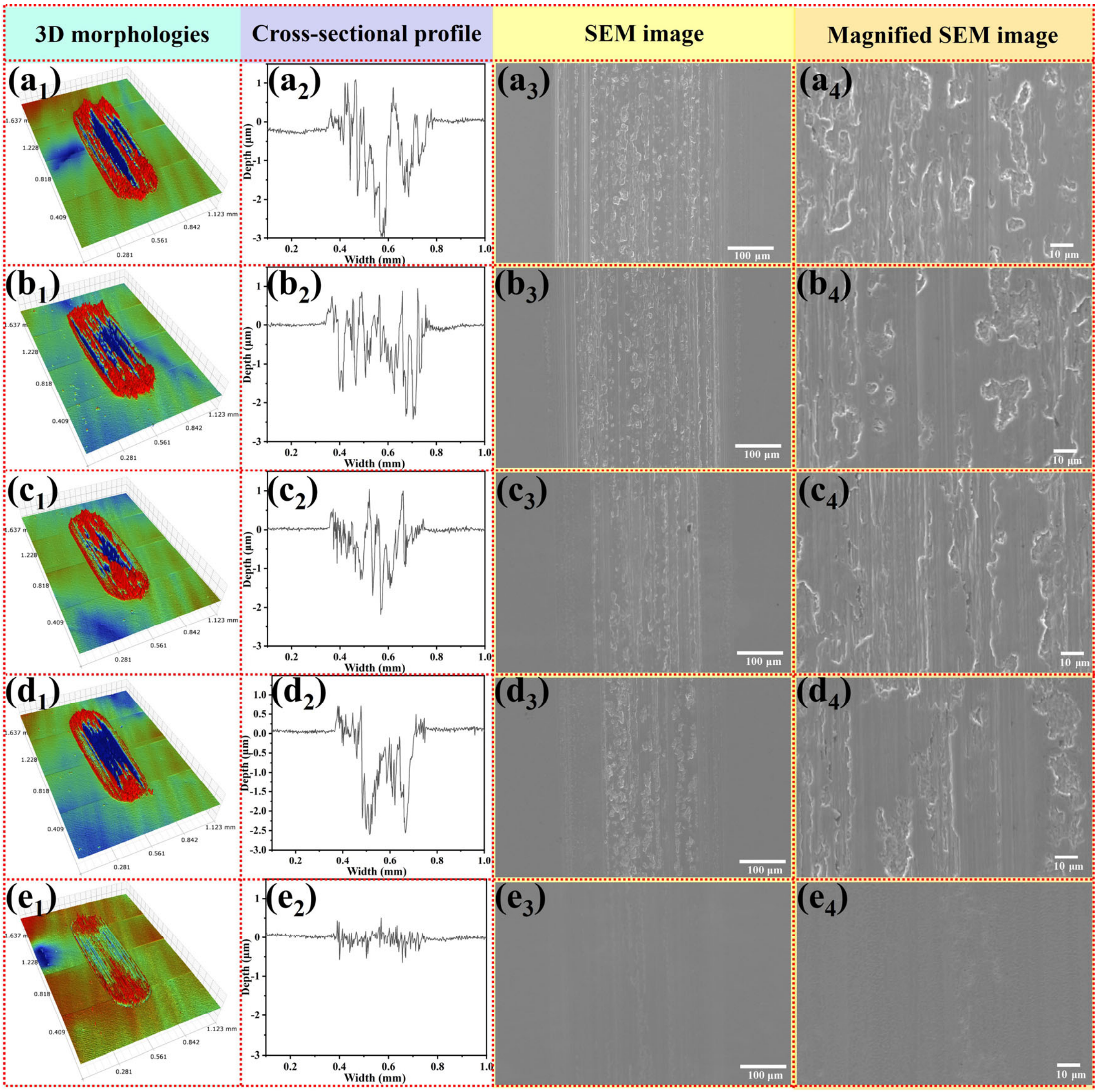

Fig. 8 3D morphologies, cross-sectional profile, and SEM images of wear tracks of (a_1–a_4) 150N, (b_1–b_4) $Ti_3C_2T_x$, (c_1–c_4) MoS_2, (d_1–d_4) $Ti_3C_2T_x/MoS_2$ mixture, and (e_1–e_4) few-layer $Ti_3C_2T_x/MoS_2$ heterojunction at the load of 140 N.

3.3 Analysis of friction mechanism

The wear situation of wear track under 150N with 0.3 wt% few-layer $Ti_3C_2T_x/MoS_2$ heterojunction lubrication were further checked by SEM with EDS to prove the existence of a uniform friction film. As shown in Fig. 9(b), Mo, S, Ti, and C are uniformly distributed on the surface of wear track. It is demonstrated for all the characterizations that the formation of deposited few-layer $Ti_3C_2T_x/MoS_2$ heterojunction on the rubbing surfaces exserts an enormous function on reducing friction and wear.

The formation of friction film benefits from good dispersion of additives in base oil. As shown in Fig. S4 in the ESM, only the few-layer $Ti_3C_2T_x/MoS_2$ heterojunction in base oil can remain dispersible stability after 4 d, while other additives have completely precipitated after 4 d. The vertically grown MoS_2 has a steric hindrance effect and inhibits the agglomeration of Ti_3C_2 nanosheets [48]. In the meantime, few-layer $Ti_3C_2T_x$ nanosheets provide growth sites for MoS_2 to keep MoS_2 away from agglomerating into a spherical shape (Fig. 2(b) and Fig. S1 in the ESM).

The XPS spectrum of the worn surface lubricated with few-layer $Ti_3C_2T_x/MoS_2$ heterojunction was investigated to further make clear the lubrication

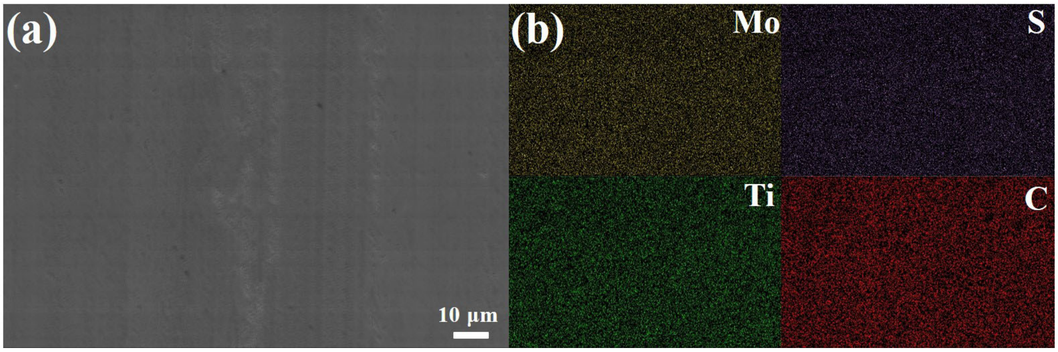

Fig. 9 (a) SEM and (b) mapping of the tribofilm lubricated with few-layer $Ti_3C_2T_x/MoS_2$ heterojunction.

mechanism. The full-scale XPS pattern from the binding energy of 0 to 800 eV and the fitted XPS fine spectra of Fe 2p, O 1s, Mo 3d, S 2p, and Ti 2p on the wear track are shown in Fig. 10. The full spectrum in Fig. 10(a) shows not only the predominant Fe and O elements, but also the presence of Mo, S, Ti, and C elements, which was consistent with the result of mapping in Fig. 9(b). As shown in Figs. 10(b) and 10(e), the Fe_2O_3 and FeO signals in Fe 2p and O 1s peaks indicate that some Fe elements have been oxidized during the friction process [49]. Furthermore, the $FeSO_4$ signals in Fe 2p peak (Fig. 10(b)) and S 2p peak (Fig. 10(d)) illustrate that the Fe and S elements can have chemical reaction to form a new friction protection film [31, 50]. The XPS spectra of Mo 3d shown in Fig. 10(c) is composed of four peaks corresponding to MoS_2 (230.1 and 233.6 eV) and MoO_3 (234.5 and 236.8 eV), respectively [51]. Ti 2p peak (Fig. 10(f)) is composed of Ti–O bonding and Ti–C bonding [52]. Therefore, the above XPS analysis is inferred that the few-layer $Ti_3C_2T_x/MoS_2$ heterojunction can be deposited on the rubbed surface and form an adsorption film. The adsorption film is mainly composed of MoS_2 and few-layer $Ti_3C_2T_x$, which can be determined from the peaks of Mo 3d, S 2p, and Ti 2p. Then, due to the friction-heat and high pressure of the sliding surfaces, the part of adsorption film is converted into the tribofilms which are composed of MoO_3, $FeSO_4$, iron oxide, and compound containing the C–O bonding on the lubricated metal surface. The tribo-film is strongly adsorbed on the worn surface to protect the friction interface and plays an effective

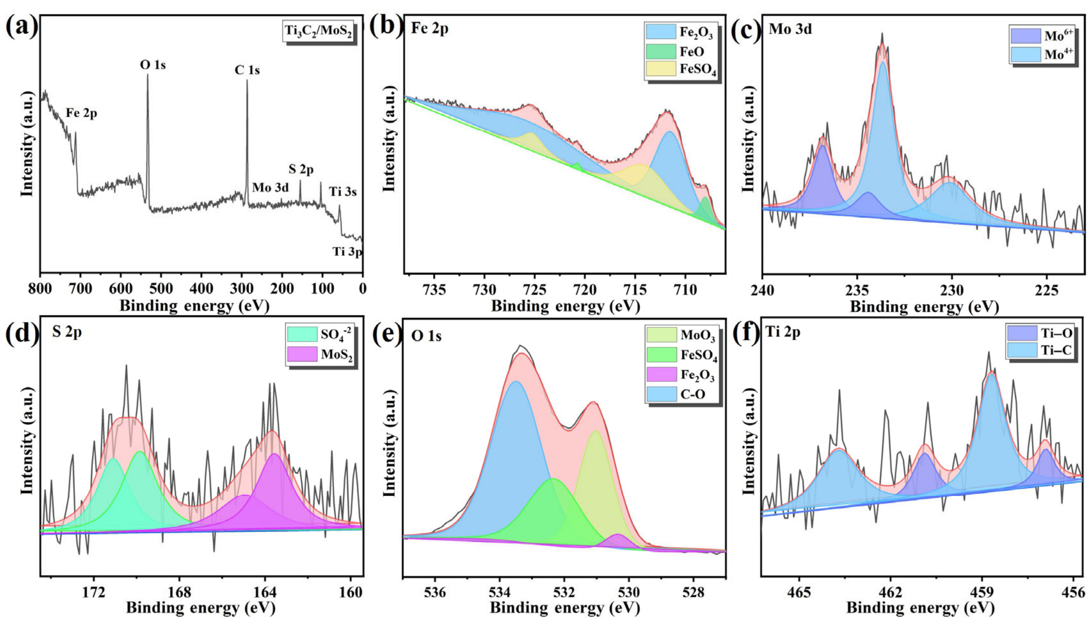

Fig. 10 XPS spectra of (a) fully scanned spectra, (b) Fe 2 p, (c) Mo 3d, (d) S 2p, (e) O 1s, and (f) Ti 2p on the surface of wear track lubricated with few-layer $Ti_3C_2T_x/MoS_2$ heterojunction dispersed 150N.

role on reducing friction and wear.

In order to determine the structural transformation of additives, the SEM with EDS mapping analysis of the wear debris was observed in Fig. 11. EDS mapping shows that Mo, S, Ti, and C are uniformly distributed on the nanosheets of wear debris collected from the wear track, indicating that the wear debris is the few-layer $Ti_3C_2T_x/MoS_2$ heterojunction. Compared with the prepared few-layer $Ti_3C_2T_x/MoS_2$ heterojunction (Fig. 2(c)), the local regions of MoS_2 nanosheets on the surface of few-layer $Ti_3C_2T_x/MoS_2$ heterojunction evolved from a vertical to a parallel arrangement after friction. The change in this arrangement contributes to the exfoliation of the MoS_2 nanosheets from the few-layer $Ti_3C_2T_x/MoS_2$ heterojunction during the rubbing process, and leading to exfoliated small size MoS_2 nanosheets to penetrate into the pits and valleys of the reciprocating surfaces and reducing the direct contact with metal surfaces [53].

Here, the lubrication mechanisms of few-layer $Ti_3C_2T_x/MoS_2$ heterojunction as an additive in the 150N base oil can be described in Fig. 12. In the running-in phase of friction, owing to the good dispersion given by the steric hindrance effect of heterojunctions, the few-layer $Ti_3C_2T_x/MoS_2$ heterojunction in oil can be continuously entered and deposited in the contact area. Then, under pressure and shear action, the vertical arrangement of MoS_2 nanosheets is transformed into parallel arrangement, and separated from the $Ti_3C_2T_x$ nanosheets. The separated small size MoS_2 nanosheets penetrate into the contact area and gradually deposit in the asperities of the reciprocating surfaces to form a more dense and uniform friction film. The larger $Ti_3C_2T_x$ nanosheets can fill up the pits and valleys and make the contact surface smoother. In the process of friction, the applied load at rapid reciprocating movement produces high temperature and pressure, which leads to the damage of thin adsorption film. Under high temperature and pressure action, the deposited few-layer $Ti_3C_2T_x/MoS_2$ heterojunction will go through complicated tribo-chemical reactions, which forms a new chemical

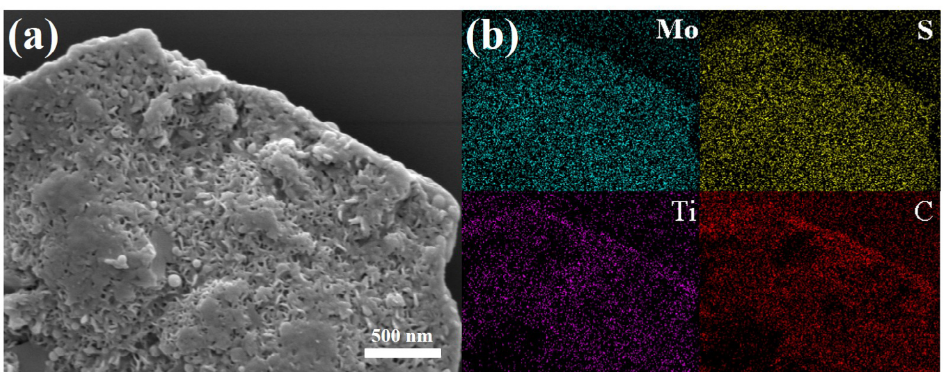

Fig. 11 (a) SEM images and (b) mapping results of few-layer $Ti_3C_2T_x/MoS_2$ heterojunction debris after friction.

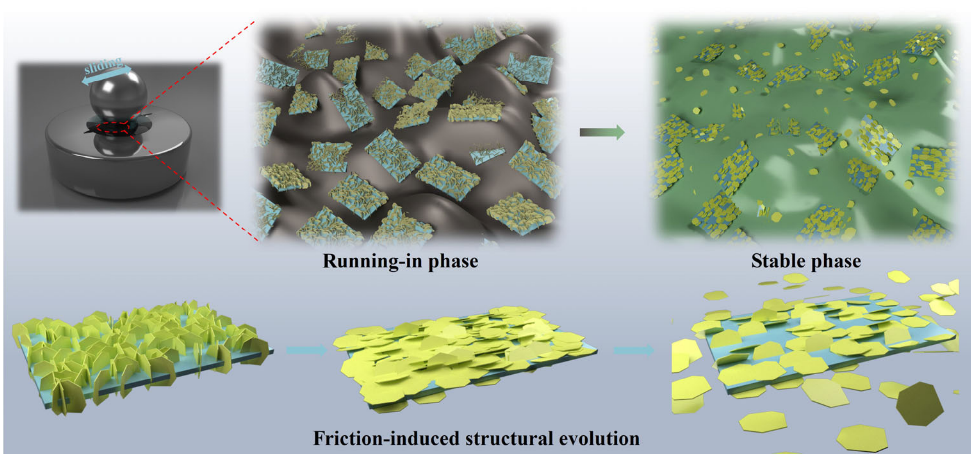

Fig. 12 Schematic diagram about the lubrication mechanisms of few-layer $Ti_3C_2T_x/MoS_2$ heterojunction.

transfer film and improves the interaction of friction-interfaces. In conclusion, the excellent lubrication performance of few-layer $Ti_3C_2T_x/MoS_2$ heterojunction benefits from the synergistic lubrication effect.

4 Conclusions

The lubrication behavior of few-layer $Ti_3C_2T_x/MoS_2$ heterojunction as oil additives was studied. The lubrication mechanism was investigated by analyzing the chemical nature, morphology of wear debris and wear track. The significant conclusions are elucidated as follows.

(1) Few-layer $Ti_3C_2T_x/MoS_2$ heterojunction was prepared through hydrothermal method. MoS_2 nanosheets are vertically and uniformly grown on the surface of few-layer $Ti_3C_2T_x$ owing to the interaction between the oxygen-containing functional groups of the few-layer $Ti_3C_2T_x$ and Mo precursor.

(2) The lubrication performances of few-layer $Ti_3C_2T_x/MoS_2$ heterojunction is superior to those of few-layer $Ti_3C_2T_x$, MoS_2, or their mixture. The introduction of 0.3 wt% few-layer $Ti_3C_2T_x/MoS_2$ heterojunction into 150N can reduce friction coefficient and wear volumes by 38.85% and 83.52%, respectively.

(3) The unique heterojunction structure with good dispersion and the friction-induced evolution of $Ti_3C_2T_x/MoS_2$ heterojunction are beneficial to give full play of synergistic lubrication.

(4) The $Ti_3C_2T_x/MoS_2$-deposited film and tribo-chemical film composed of MoO_3, $FeSO_4$, iron oxide, and compound can enhance the interaction of sliding interfaces, thereby effectively reducing the friction and wear.

Acknowledgements

The authors gratefully acknowledge the financial support provided by National Natural Science Foundation of China (No. 52075458) and Sichuan Science and Technology Program (No. 2021JDRC0094). Meanwhile, the authors gratefully acknowledge Analytical and Testing Center of Southwest Jiaotong University for supporting the SEM measurements.

Electronic Supplementary Material: Supplementary material is available in the online version of this article at https://doi.org/10.1007/s40544-021-0568-3.

References

[1] Bronshteyn L A, Kreiner J H. Energy efficiency of industrial oils. *Tribol Trans* **42**(4): 771–776 (1999)

[2] Holmberg K, Andersson P, Nylund N O, Mäkelä K, Erdemir A. Global energy consumption due to friction in trucks and buses. *Tribol Int* **78**: 94–114 (2014)

[3] Holmberg K, Kivikytö-Reponen P, Härkisaari P, Valtonen K, Erdemir A. Global energy consumption due to friction and wear in the mining industry. *Tribol Int* **115**: 116–139 (2017)

[4] Taylor R I. Tribology and energy efficiency: From molecules to lubricated contacts to complete machines. *Faraday Discuss* **156**: 361–382 (2012)

[5] Wu Y Y, Tsui W C, Liu T C. Experimental analysis of tribological properties of lubricating oils with nanoparticle additives. *Wear* **262**(7–8): 819–825 (2007)

[6] Lee K, Hwang Y, Cheong S, Choi Y, Kwon L, Lee J, Kim S H. Understanding the role of nanoparticles in nano-oil lubrication. *Tribol Lett* **35**(2): 127–131 (2009)

[7] Han Y Y, Qiao D, Sun L M, Feng D P. Functional alkylimidazolium ionic liquids as lubricants for steel/aluminum contact: Influence of the functional groups on tribological performance. *Tribol Int* **119**: 766–774 (2018)

[7] Han Y, Qiao D, Sun L, Feng D. Functional alkylimidazolium ionic liquids as lubricants for steel/aluminum contact: Influence

of the functional groups on tribological performance. *Tribol Int* **119**: 766–774 (2018)

[8] Trachsel M, Pittini R, Dual J. Evaluation and quantification of friction using Ionic Liquids in small, self lubricating journal bearings. *Tribol Int* **122**: 15–22 (2018)

[9] Ahmed N S, Nassar A M, Nasser R M, Khattab A F, Abdel-Azim A A A. Synthesis and evaluation of some polymers as lubricating oil additives. *J Dispers Sci Technol* **33**(5): 668–675 (2012)

[10] Fan X, Wang P. High-performance lubricant additives based on modified graphene oxide by ionic liquids. *J Colloid Interface Sci* **452**: 98–108 (2015)

[11] Xiao H, Liu S. 2D nanomaterials as lubricant additive: A review. *Mater Des* **135**: 319–332 (2017)

[12] Gan C, Liang T, Li X, Li W, Li H, Fan X Q, Zhu M. Ultra-dispersive monolayer graphene oxide as water-based lubricant additive: Preparation, characterization and lubricating mechanisms. *Tribol Int* **155**: 106768 (2021)

[13] Pawlak Z, Kaldonski T, Pai R, Bayraktar E, Oloyede A. A comparative study on the tribological behaviour of hexagonal boron nitride (h-BN) as lubricating micro-particles—An additive in porous sliding bearings for a car clutch. *Wear* **267**(5–8): 1198–1202 (2009)

[14] Naguib M, Kurtoglu M, Presser V, Lu J, Niu J J, Heon M, Hultman L, Gogotsi Y, Barsoum M W. Two-dimensional nanocrystals produced by exfoliation of Ti_3AlC_2. *Adv Mater* **23**(37): 4248–4253 (2011)

[15] Cai M, Yan H, Li Y T, Li W, Li H, Fan X Q, Zhu M H. $Ti_3C_2T_x$/PANI composites with tunable conductivity towards anticorrosion application. *Chem Eng J* **410**: 128310 (2021)

[16] Chang T H, Zhang T, Yang H, Li K, Tian Y, Lee J Y, Chen P Y. Controlled crumpling of two-dimensional titanium carbide (MXene) for highly stretchable, bendable, efficient supercapacitors. *ACS Nano* **12**(8): 8048–8059 (2018)

[17] Chen Y, Xie X, Xin X, Tang ZR, Xu YJ. $Ti_3C_2T_x$-based three-dimensional hydrogel by a graphene oxide-assisted self-convergence process for enhanced photoredox catalysis. *ACS Nano* **13**(1): 295–304 (2019)

[18] Naguib M, Mochalin V N, Barsoum M W, Gogotsi Y. 25th anniversary article: MXenes new family of two-dimensional materials. *Adv Mater* **26**(7): 992–1005 (2014)

[19] Shahzad F, Alhabeb M, Hatter C B, Anasori B, Man Hong S, Koo C M, Gogotsi Y. Electromagnetic interference shielding with 2D transition metal carbides (MXenes). *Science* **353**(6304): 1137–1140 (2016)

[20] Xie X Q, Chen C, Zhang N, Tang Z R, Jiang J J, Xu Y J. Microstructure and surface control of MXene films for water purification. *Nat Sustain* **2**(9): 856–862 (2019)

[21] Yan H, Cai M, Li W, Fan X Q, Zhu M H. Amino-functionalized $Ti_3C_2T_x$ with anti-corrosive/wear function for waterborne epoxy coating. *J Mater Sci Technol* **54**: 144–159 (2020)

[22] Zhang X, Xue M, Yang X, Wang Z, Luo G, Huang Z, Sui X, Li C. Preparation and tribological properties of $Ti_3C_2(OH)_2$ nanosheets as additives in base oil. *RSC Adv* **5**(4): 2762–2767 (2015)

[23] Liu Y, Zhang X, Dong S, Ye Z, Wei Y. Synthesis and tribological property of $Ti_3C_2T_x$ nanosheets. *J Mater Sci* **52**(4): 2200–2209 (2017)

[24] Nguyen H T, Chung K H. Assessment of tribological properties of Ti_3C_2 as a water-based lubricant additive. *Materials* **13**(23): 5545 (2020)

[25] Zhao J, Mao J, Li Y, He Y, Luo J. Friction-induced nano-structural evolution of graphene as a lubrication additive. *Appl Surf Sci* **434**: 21–27 (2018)

[26] Kim D, Ko T Y, Kim H, Lee G H, Cho S, Koo C M. Nonpolar organic dispersion of 2D $Ti_3C_2T_x$ MXene flakes *via* simultaneous interfacial chemical grafting and phase transfer method. *ACS Nano* **13**(12): 13818–13828 (2019)

[27] Chen Z, Liu Y H, Gunsel S, Luo J B. Mechanism of antiwear property under high pressure of synthetic oil-soluble ultrathin MoS_2 sheets as lubricant additives. *Langmuir* **34**(4): 1635–1644 (2018)

[28] Tomala A, Ripoll M R, Kogovšek J, Kalin M, Bednarska A, Michalczewski R, Szczerek M. Synergisms and antagonisms between MoS_2 nanotubes and representative oil additives under various contact conditions. *Tribol Int* **129**: 137–150 (2019)

[29] Wu X H, Gong K L, Zhao G Q, Lou W J, Wang X B, Liu W M. Surface modification of MoS_2 nanosheets as effective lubricant additives for reducing friction and wear in poly-α-olefin. *Ind Eng Chem Res* **57**(23): 8105–8114 (2018)

[30] Chouhan A, Sarkar T K, Kumari S, Vemuluri S, Khatri O P. Synergistic lubrication performance by incommensurately stacked ZnO-decorated reduced graphene oxide/MoS_2 heterostructure. *J Colloid Interface Sci* **580**: 730–739 (2020)

[31] Gong K L, Wu X H, Zhao G Q, Wang X B. Nanosized MoS_2 deposited on graphene as lubricant additive in polyalkylene glycol for steel/steel contact at elevated temperature. *Tribol Int* **110**: 1–7 (2017)

[32] Zhao J, He Y Y, Wang Y F, Wang W, Yan L, Luo J B. An investigation on the tribological properties of multilayer graphene and MoS_2 nanosheets as additives used in hydraulic applications. *Tribol Int* **97**: 14–20 (2016)

[33] Alhabeb M, Maleski K, Anasori B, Lelyukh P, Clark L, Sin S, Gogotsi Y. Guidelines for synthesis and processing of two-dimensional titanium carbide ($Ti_3C_2T_x$ MXene). *Chem Mater* **29**(18): 7633–7644 (2017)

[34] Zhang J H, Xing C, Shi F. MoS_2/Ti3C2 heterostructure for

efficient visible-light photocatalytic hydrogen generation. *Int J Hydrog Energy* **45**(11): 6291–6301 (2020)
[35] Lukatskaya M R, Mashtalir O, Ren C E, Dall'Agnese Y, Rozier P, Taberna P L, Naguib M, Simon P, Barsoum M W, Gogotsi Y. Cation intercalation and high volumetric capacitance of two-dimensional titanium carbide. *Science* **341**(6153): 1502–1505 (2013)
[36] Lipatov A, Alhabeb M, Lukatskaya M R, Boson A, Gogotsi Y, Sinitskii A. Effect of synthesis on quality, electronic properties and environmental stability of individual monolayer Ti_3C_2 MXene flakes. *Adv Electron Mater* **2**(12): 1600255 (2016)
[37] Ghidiu M, Lukatskaya M R, Zhao M Q, Gogotsi Y, Barsoum M W. Conductive two-dimensional titanium carbide 'clay' with high volumetric capacitance. *Nature* **516**(7529): 78–81 (2014)
[38] Wang G, Zhang J, Yang S, Wang F X, Zhuang X D, Müllen K, Feng X L. Vertically aligned MoS_2 nanosheets patterned on electrochemically exfoliated graphene for high-performance lithium and sodium storage. *Adv Energy Mater* **8**(8): 1702254 (2018)
[39] Xiu L, Wang Z, Yu M, Wu X, Qiu J. Aggregation-resistant 3D MXene-based architecture as efficient bifunctional electrocatalyst for overall water splitting. *ACS Nano* **12**(8): 8017–8028 (2018)
[40] Zhang X, Zhang Z H, Zhou Z. MXene-based materials for electrochemical energy storage. *J Energy Chem* **27**(1): 73–85 (2018)
[41] Chandran M, Thomas A, Raveendran A, Vinoba M, Bhagiyalakshmi M. MoS_2 confined MXene heterostructures as electrode material for energy storage application. *J Energy Storage* **30**: 101446 (2020)
[42] Wang X, Li H, Li H, Lin S, Ding W, Zhu X G, Sheng Z G, Wang H, Zhu X B, Sun Y P. 2D/2D 1T-MoS_2/Ti_3C_2 MXene heterostructure with excellent supercapacitor performance. *Adv Funct Mater* **30**(15): 0190302 (2020)
[43] Li J H, Rui B L, Wei W X, Nie P, Chang L M, Le Z Y, Liu M Q, Wang H R, Wang L M, Zhang X G. Nanosheets assembled layered MoS_2/MXene as high performance anode materials for potassium ion batteries. *J Power Sources* **449**: 227481 (2020)
[44] Jiao S L, Liu L. Friction-induced enhancements for photocatalytic degradation of MoS_2@Ti_3C_2 nanohybrid. *Ind Eng Chem Res* **58**(39): 18141–18148 (2019)
[45] Rodriguez A, Jaman M S, Acikgoz O, Wang B, Yu J, Grützmacher P G, Rosenkranz A, Baykara M Z. The potential of $Ti_3C_2T_x$ nano-sheets (MXenes) for nanoscale solid lubrication revealed by friction force microscopy. *Appl Surf Sci* **535**: 147664 (2021)
[46] Huang H D, Tu J P, Zou T Z, Zhang L L, He D N. Friction and wear properties of IF–MoS_2 as additive in paraffin oil. *Tribol Lett* **20**(3–4): 247–250 (2005)
[47] Liu L, Zhou W. MoS_2 hollow microspheres used as a green lubricating additive for liquid paraffin. *Tribol Int* **114**: 315–321 (2017)
[48] Hou K M, Wang J Q, Yang Z G, Ma L M, Wang Z F, Yang S R. One-pot synthesis of reduced graphene oxide/molybdenum disulfide heterostructures with intrinsic incommensurateness for enhanced lubricating properties. *Carbon* **115**: 83–94 (2017)
[49] Meng Y, Su F H, Chen Y Z. A novel nanomaterial of graphene oxide dotted with Ni nanoparticles produced by supercritical CO_2-assisted deposition for reducing friction and wear. *ACS Appl Mater Interfaces* **7**(21): 11604–11612 (2015)
[50] Xu Y F, Peng Y B, Dearn K D, Zheng X J, Yao L L, Hu X G. Synergistic lubricating behaviors of graphene and MoS_2 dispersed in esterified bio-oil for steel/steel contact. *Wear* **342–343**: 297–309 (2015)
[51] Hu K H, Wang J, Schraube S, Xu Y F, Hu X G, Stengler R. Tribological properties of MoS_2 nano-balls as filler in polyoxymethylene-based composite layer of three-layer self-lubrication bearing materials. *Wear* **266**(11–12): 1198–1207 (2009)
[52] Xu X S, Sun B T, Liang Z Q, Cui H Z, Tian J. High-performance electrocatalytic conversion of N_2 to NH_3 using 1T–MoS_2 anchored on Ti_3C_2 MXene under ambient conditions. *ACS Appl Mater Interfaces* **12**(23): 26060–26067 (2020)
[53] Tannous J, Dassenoy F, Lahouij I, Mogne T, Vacher B, Bruhács A, Tremel W. Understanding the tribochemical mechanisms of IF–MoS_2 nanoparticles under boundary lubrication. *Tribol Lett* **41**(1): 55–64 (2011)

Peng FENG. He is currently a postgraduate student at School of Materials Science and Engineering, Southwest Jiaotong University, China. His research interests include high dispersion of lubricating materials and the tribological properties of lubricating additives.

Yanping REN. He received his bachelor degree in mechanical engineering in 2015 from Mechanical Engineering School at Southwest Jiaotong University. Recently, he is studying for a Ph.D. degree at Tribology Research Institute at Southwest Jiaotong University. His research interests are in fretting wear, fretting fatigue, and testing equipment development.

Yuting LI. She is currently a Ph.D. candidate at School of Materials Science and Engineering, Southwest Jiaotong University. Her research interests include design of lubricating materials and tribological properties of novel deep eutectic solvents.

Jifan HE. He received his bachelor degree in mechanical engineering in 2015 from Northwest Agriculture & Forestry University, Xi'an, China. He is currently pursuing his Ph.D. at Tribology Research Institute, Southwest Jiaotong University. His research interests include fretting tribology, the development of fretting apparatus, and electromechanical equipment

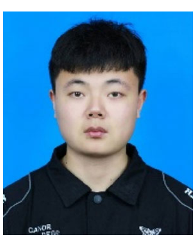

Zhuang ZHAO. He is a postgraduate student at School of Materials Science and Engineering, Southwest Jiaotong University. His research interests include high dispersion of graphene additives in synthetic oils and excellent tribological properties.

Xiaoliang MA. He received his bachelor degree from Shandong University of Science and Technology, China, in 2019. He is currently a graduate student at School of Materials Science and Engineering, Southwest Jiaotong University. His research interests include design of lubricating materials and tribological properties of lubricant additives.

Xiaoqiang FAN. He received his bachelor degree in 2011 from Qingdao University of Science & Technology and Ph.D. degree from Lanzhou Institute of Chemical Physics, Chinese Academy of Sciences in 2016. He is currently an associate professor at Southwest Jiaotong University. His research focuses on lubricating materials, corrosion protection, and engineering applications. He has published over 60 papers in international journals, which received more than 700 citations.

Minhao ZHU. He received his bachelor and master degrees from Southwest Jiaotong University, Sichuan, China, in 1990 and 1993, respectively. Then he has been working in Southwest Jiaotong University. From 1996 to 2001, he pursued his Ph.D. from Southwest Jiaotong University, Sichuan, China. His current position is a professor, doctoral supervisor, and dean of School of Materials Science and Engineering. His research areas cover fretting wear, fretting fatigue, surface engineering, and design of fastener connection. He has published over 200 papers in international journals such as *Carbon*, *Tribology International*, *Surface & Coatings Technology*, *Tribology Letters*, *Wear, and Friction*, etc., which received more than 1,000 citations.